Journal of Population Therapeutics & Clinical Pharmacology

EVALUATING TIO2 NANOPARTICLE CATALYSTS ON ZSM-5 ZEOLITE FOR TEXTILE WASTEWATER REMEDIATION AND HYDROGEN PRODUCTION

Nida Aslam[1], Hafiza Hamna Arif [2], Md Mahbubur Rahman [3], Sadia Batool[4], Yaseen[5], Sadia Khalid [6], Bryan O. Oyarebu[7], Nida Shehbaz [8]

[1]Student, Department of Chemistry, The University of Lahore, Sargodha Campus, Pakistan, Email: aa4060@gmail.com

[2]Student, Department of Chemistry, The University of Lahore, Sargodha Campus, Pakistan, Email: hamnac19@gmail.com

[3]Department of Industrial and Systems Engineering, Lamar University, Texas, USA, Email: mrahman41@lamar.edu

[4]Student, Department of Chemistry, The University of Lahore, Sargodha Campus, Pakistan, Email: sadiarana168@gmail.com

[5]Department of chemistry, Quaid-i-Azam University, Islamabad 45320, Pakistan, Email: yaseenwali978@gmail.com

[6]Student, Department of Chemistry, The University of Lahore, Sargodha Campus, Pakistan, Email: sadiakhalid162@gmail.com

[7]American Medical Association, Department of Medicine, Georgetown University School of Medicine, U.S.A, Email: boyarebu@tulane.edu

[8]Student, Department of Chemistry, The University of Lahore, Sargodha Campus, Pakistan, Email: nidamalik@gmail.com

ABSTRACT:

Background: Advanced Oxidative Processes (AOPs), particularly photocatalysis, have gained attention for their potential in environmental remediation and energy production. This study explores the integration of photocatalytic degradation of synthetic textile waste with hydrogen production, using titanium dioxide (TiO2) nanoparticles supported on ZSM-5 zeolite.

Methods: TiO2 nanoparticles were deposited on ZSM-5 zeolite with 5% and 10% active phases by weight. The resulting catalysts were characterized for their textural, molecular, and morphological properties. Photocatalytic experiments were conducted in a batch reactor with a recycling system, using reactive blue dye RB250 as a model pollutant under artificial UV radiation.

Results: The supported TiO2 catalysts demonstrated rapid decolorization of RB250, achieving complete color removal within minutes of UV irradiation. Further analysis revealed over 80%

mineralization of the wastewater for all catalyst types. Hydrogen production was also assessed, with the pure industrial TiO2 catalyst outperforming the zeolite-supported variants. Specifically, the industrial catalyst produced 11.05 µmol of H2 per gram of catalyst, 50% more effective than the supported catalysts with 5 and 10% active phases.

Conclusion: TiO2-based nanoparticle catalysts effectively decolor textile wastewater and produce hydrogen. While the zeolite-supported catalysts were slightly less efficient in hydrogen production, they still showed significant potential for dual-purpose environmental remediation and renewable energy applications. Future studies could explore optimizing catalyst composition and operational parameters to enhance degradation and hydrogen yield.

KEYWORDS: Photocatalysis, Dye, Hydrogen, Titanium Dioxide, ZSM-5.

KEYWORDS: Dye, Hydrogen, Photocatalysis, ZSM-5, and Titanium Dioxide.

INTRODUCTION:

As the concern for the environment grows, there are stricter controls on the emissions of textile industry waste because some types of dyes are harmful, can cause cancer, and make it hard for living things to break down. At the same time, people are looking for alternative energy sources to fossil fuels since most of the hydrogen made in the world comes from nonrenewable sources.

In this case, heterogeneous photocatalysis with titanium photocatalyst is a technology that is quickly growing for treating wastewater and making hydrogen because it is safe for the environment and can use sunlight as a power source (Kandhasamy et al., 2024; Sukarta & Sastrawidana, 2024).

Photocatalytic treatment of effluent and hydrogen production is hopeful, but it still needs improvement. This can be done by making new, more active catalysts and improving many other aspects of the process. Titanium dioxide is a famous and promising photocatalyst that produces hydrogen and removes harmful organic pollutants. It is also economically viable, non-toxic, biologically inert, and resistant to high temperatures. It's important to note that these catalysts' band gap energies (3.2 eV for anatase and 3.0 eV for the rutile phase) can change based on how they were made (Nagaraja, Arun Pandian & Oh, 2024; Rohit et al., 2024).

The problem with this catalyst is that the photogenerated electron-hole pairs recombine quickly, which limits the photoreactivity to the UV area. This makes it hard to use in industry, and it's also hard to get back to normal after the process. Doping titanium with transition metals

or organic dyes that can increase its absorption properties to the visible range and immobilize it on suitable supports that can stop charge recombination and ensure these catalysts work well again is a successful way to get around these problems. The supports need to be able to let UV light through, not change how the catalyst works, have a lot of surface area, not react chemically, and be able to adsorb things (Adesibikan, Emmanuel, Olawoyin, & Ndungu, 2024; Sathisha, Krishnamurthy, Harini, & Nagaraju, 2024).

Zeolites like ZSM-5 can make catalysts work better when used in this way. Zeolites have a lot of surface area and can be either hydrophobic or hydrophilic. They also have acidic active sites that can be controlled based on the need, pores compatible with most raw materials, shape selectivity, reagent selectivity, products, and transition state. This work aimed to make a catalyst that can do more than one thing. The color must be removed from the reactive blue dye RB 250, and photocatalysis is used to produce hydrogen (Doan et al., 2024; Shreelakshmi et al., 2024).

EXPERIMENTAL:

IMPREGNATION:

Wet impregnation was used to make catalysts with 5 and 10 wt% TiO2 following a modified method suggested by Park et al. After being dried in an oven for 24 hours, 9 grams of support were weighed and put into a volumetric flask with 70 milliliters of isopropyl alcohol. The mixture was then stirred with a magnet for 30 minutes. Once the solution was mixed entirely, it was put inside a slit bag in an atmosphere of harmless N2. Then, 3.8 mL of titanium isopropoxide was included and heated over high heat for one hour in a sand bath that had already been heated to 100°C (Krishnan et al., 2024; Lee, Danish, & Jo, 2024).

The condenser was then removed, and the solution was mixed until the solvent disappeared. The solution was dried out in an oven at 100°C for 12 hours, or until it looked like paste. A pelletizer puts 1.5 tons of pressure on this material to make pellets. The pellets were then heated at 500°C for 5 hours. Sieves with openings between 80 mm and 100 mm were used to change the particle size, and the mixture was then heated to 500°C (Chandiran et al., 2024; Shabna, Singh, Dhas, Jeyakumar, & Biju, 2024).

CHARACTERIZATION OF THE CATALYSTS:

We used atomic absorption spectrometry, N2 adsorption isotherms, X-ray diffraction (XRD), FTIR, DTP-NH3, photoacoustic absorption, and point of zero charge (pHZPC) spectroscopy to study the catalysts that were made in this study (Dhanda, Nain, & Dahiya, 2024).

REACTIONAL UNITS:

A recycling rate batch reactor was used to test how well the RB 250 dye could be removed from things. This had a 700 mL beaker that was modified to have an inlet at the bottom and an outlet at the top. A thermostatic bath cooled it, and a centrifugal pump controlled the recycling rate. The reactor also had ten ppm of coloring solution and 1 gL-1 catalyst. The solution was stirred in the dark for an hour for each test to see what would happen with adsorption (Prathap, Naik, Viswanath, & Vishnu, 2024; Wani et al., 2024).

It was then exposed to light and broken down over 5 hours, with portions taken regularly. These were then filtered through a 0.22 μm Millipore membrane while studied using UV spectrophotometry. The wavelength of 617 nm was used to measure how much dye was in the mix. To test the photocatalytic system, processes to make hydrogen from photolysis of water were performed in a cylinder-shaped stainless steel reactor that held 1 liter of liquid and a 7-watt UV lamp (Gharbi et al., 2024; Patar, Mittal, Bhuyan, & Borthakur, 2024).

Water, ethanol (10% as a sacrifice reagent), and 900 mg of catalyst were put into the reactor to start the reaction. Before the light was turned on, 10 ml/min of argon gas was bubbled using the solution for 20 minutes to remove any oxygen in the medium. Gas samples were collected at set times to track the reaction. They were then studied using a Varian 3300 chromatograph with a thermal conductivity detector (TCD) and a Carboxen 1004 column (Basavannavar et al., 2024; Sarvalkar et al., 2024).

RESULTS AND DISCUSSION:

Table 1 shows the codes used to talk about the findings of the titanium dioxide-impregnated catalysts.

Catalysts	Reference
5% TiO2/ZSM-5	Z5
ZSM-5	Z
10% TiO2/ZSM-5	Z10

Table 1. Reference of catalysts.

Table 1: A list of catalysts.

Atomic absorption determined how many oxides were embedded in each support. In Table 2, you can see how much titanium dioxide is in each catalyst. It was seen that the triggers had values that were close to what would be expected from their theory. The BET test of the oxides mixed with ZSM-5 zeolite showed that all catalysts' total BET area decreased as the supported active phase increased. This aligns with the XRD diffractograms (Figure 2) (Liou, Liu, Liao, & Ku, 2024; Samal & Das).

As shown in Table 2, the band gap energy went down in all the samples. This is because of the plasma effect, in which semiconductor particles move into the micropores and lower the band gap energy. The particle size can change the band gap energy of semiconductors, and the samples showed the start of limiting absorption, which led to small changes in Eg and a rise in the active phase in the specimens, which could be studied (Liu et al., 2024; Pompapathi et al., 2024).

Ref	**S microbe (m2.g-1)**	**S BETa (m2.g-1)**	**Metal content**	**bandgap**
Z5	198.42	342.15	5.2%	3.12
Z	217.10	342.70	-	3.63
Z10	191.01	270.62	10.8%	3.13

When the oxide was added to the ZSM-5 zeolite (Figure 1), the typical peaks of the zeolitic structure became a little less intense. To see the catalytic supports that were filled with TiO2 at about 25° from the crystalline plane (1 0 1) of the metal oxide, which is called the anatase phase, we could see a slight increase in the diffractogram of the structure of the ZSM-5 zeolite that was filled with both 5 and 10% of the active phase in the same area. This could indicate that the metal oxide was filled into the support (Gallegos-Cerda et al., 2024; Yan et al., 2024).

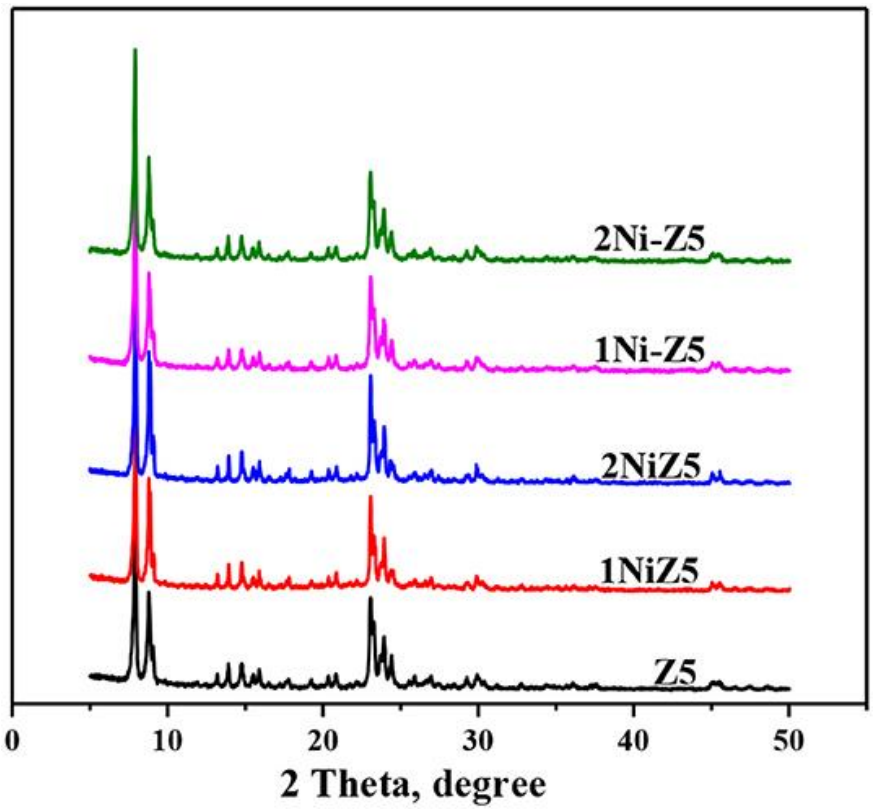

Figure 1. XRD of pure and supported catalysts.

Picture 1: XRD of pure catalysts and catalysts on a base.

In Figure 2, infrared spectroscopy (FTIR) was used to look at the crystallinity of the samples for the catalysts based on the ZSM-5 zeolite. This band at 3424 cm-1 is caused by –OH stretching. The two main hydroxyl groups are around 3639 cm-1, the structural hydroxyl groups connecting the Si-Al atoms, and 3740 cm-1, the terminal hydroxyl groups. These belong to the silanol groups (Si-OH) at 3735 cm-1 and the alumina groups (Al-OH) at 3743 cm-1 (Allawi, Mahdi, Kadhim, & Alkhayatt, 2024; Survase & Kanase, 2024).

The lack of bands between 950 and 960 cm-1 is due to the vibrational stretching of the Ti-O-Si band, which means that titanium dioxide is not incorporated into the crystalline network of the zeolite. This means that TiO2 is either spread out on the outermost layer or partially encapsulated in the cavities of the zeolite. XRD (Figure 1) shows no significant chemical association between TiO2 and ZSM-5 (Horzum, Doğan, Karaduman, & Metin, 2024; Shee & Kim, 2024).

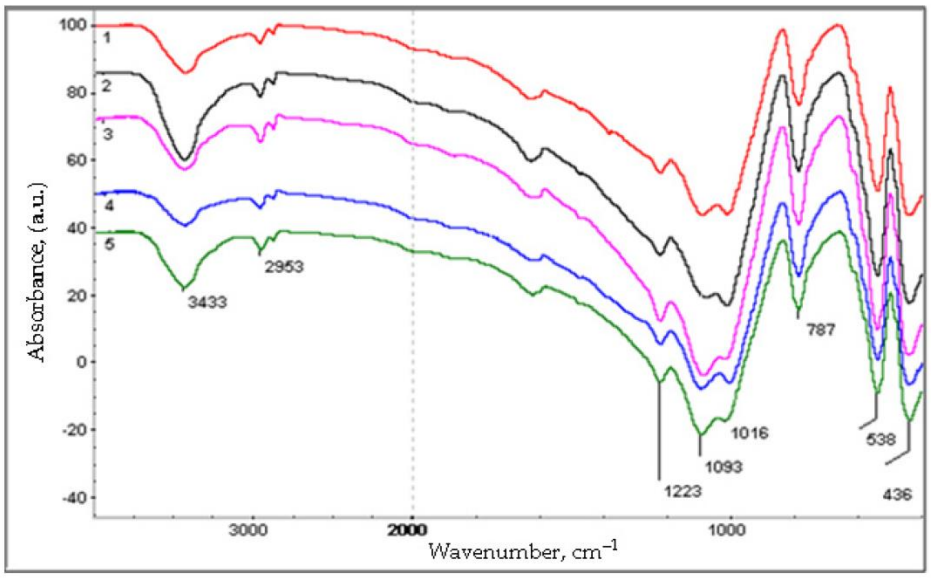

Figure 2. FTIR of supported catalysts on ZSM-5.

The FTIR of catalysts supported on ZSM-5 is shown in Figure 2.

It was found that pH changed zeolites when oxides supported them, and the desorption profile changed when various quantities of active phase content were added. Pure ZSM-5 zeolite had two sites: a weak site that got as hot as 252°C and a robust site as hot as 440°C. There was a change of acidic sites following the TiO2 impregnation process, which strengthened at lower temperatures. It's possible that the active phase, which was evenly spread on the zeolite surface and supported the XRD results, took up acidic spots after the acidity level dropped (Kumar & Kumar, 2024; Li, Zhang, Zou, Zhang, & Ma, 2024).

Figure 4 displays the photocatalytic tests for TiO2 mixed with ZSM-5 zeolite. The photocatalytic activity associated with these catalysts is higher than that of pure oxide. This may be because the oxide and zeolite work together more effectively, creating a heterojunction that increases the activity. This is mainly because fewer electron gap pair recombinations happen, causing complete charge separation (Ahlawat, Jangra, & Prakash, 2024; Masho, Arasu, Bogale, Zerrefa, & Ramamurthy, 2024).

Ref	Total Acidity (mmol NH3/g)	Main Peak Temperature (°C)	
		1st	2nd
Z5	0.719	212	350
Z	1.001	252	440
Z10	0.383	236	383

Table 3. Ammonia TPD in pure and supported zeolites

Table 3 shows the TPD of ammonia in zeolites that are pure or supported.

Table 5 shows that the ZSM-5 zeolite catalysts with a 5 and 10% TiO2 active phase changed color entirely in the first few minutes of the reaction. The 5Z catalysts changed color to 7.2 mim, and the 10Z catalysts changed color to 10.8 mim. According to Brittes et al., the difference in the percentage of the assisted active phase didn't significantly affect the efficiency. The Z5 catalyst's high photocatalytic activity is likely due to its more extensive BET area and higher proton acidity (Farahmandzadeh, Molaei, Salehi, & Molahosseini, 2024; Preethi et al., 2024).

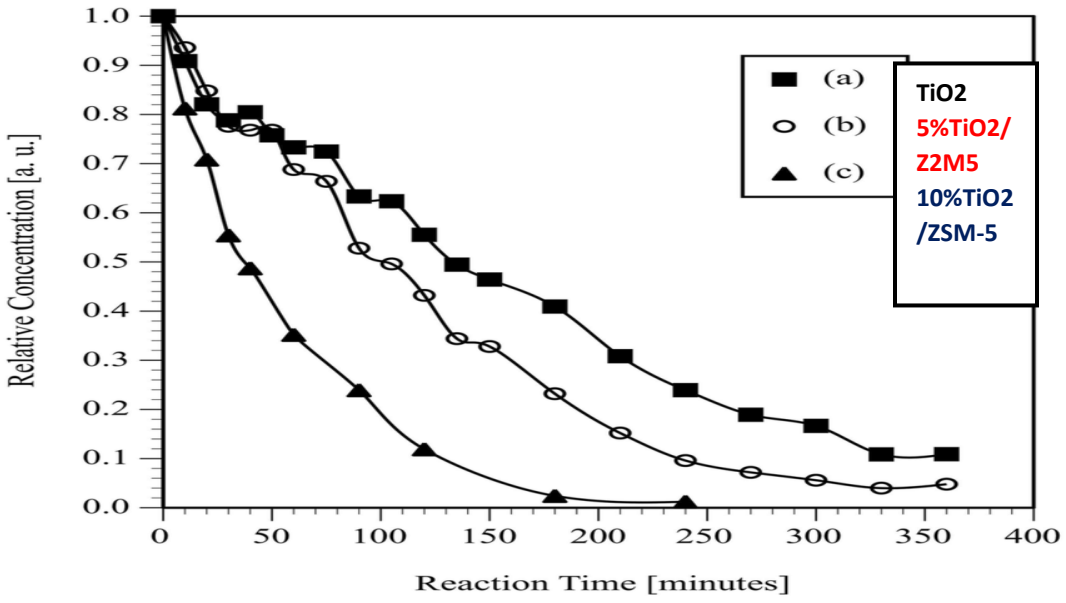

Figure 4. Photocatalytic decolorization of the reactive blue dye RB 250 with supported catalysts on ZSM-5

Figure 4: Using photocatalysis to remove the color from reactive blue dye RB 250 with ZSM-5 and catalysts

Table 4 shows the results of measuring the amount of total organic carbon (TO for the samples that were put through the recycle reactor. In general, the catalysts on the ZSM-5 zeolite made it easier for the blue dye RB250 to become minerals at a concentration of 10 ppm. Like catalysts 5A and 10A, which were not very good at photocatalysis, these could remove more than 80% of the organic molecules by mineralization (Liaquat et al., 2024; PETROVIĆ et al., 2024).

Ref.	**COT (%)**	**% Discoloration**
Z5	96.08	100
Z10	98.04	100

Table 4. Percentage of discoloration and total organic carbon (TOC) of catalysts
Table 4: The amount of discoloration and total organic carbon (TOC) in catalysts

To better understand how the dye minerals changed following the photocatalytic tests, the samples were looked at with UV-vis spectrophotometry for catalysts with 10% active phase (Figure 5). When you look at the graphs, you can see that the color has faded in the visible range (λ>350 nm). The peak at 617 nm, where the chromophore group that gives the dye its color lives, is almost gone (Chauke, Mohlala, Ngqoloda, & Raphulu, 2024).

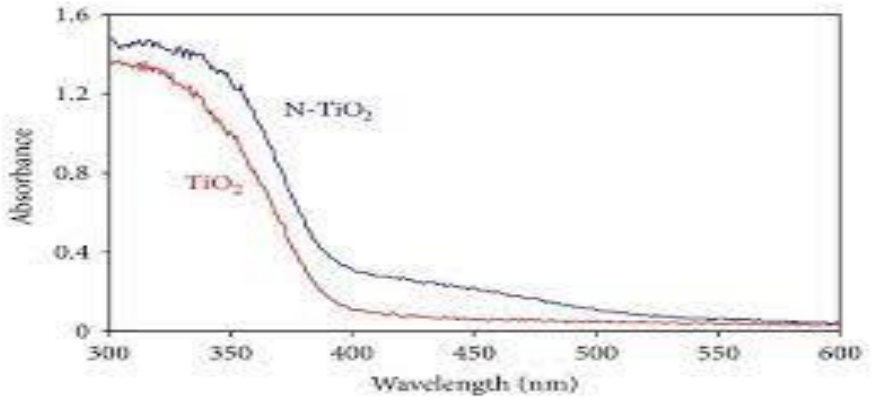

Figure 5. UV/VIS spectrum of the pure dye and samples after treatment with TiO2-supported catalysts.

Figure 5: The UV/VIS spectrum of the pure dye and the samples treated with catalysts based on TiO2.

The peak drop at 617 nm frequency shows that the dye quickly loses color when it reacts with the azo group. This drop is substantial because it means that the double bond (-N=N-) of the dyes that contain the azo group is broken, which is the best place for an oxidative attack.

In Figure 6, you can see that the catalysts weren't very good at making hydrogen. This is because commercial TiO2 worked better than the oxide mixed in with ZSM-5 zeolite, producing 11.0521 µmol H2.gcat-1 compared to 5.866 and 5.110 µmol H2.gcat-1 for the 5Z and 10Z catalysts, respectively (Xu, Guo, Xu, Shen, & Zhao, 2024).

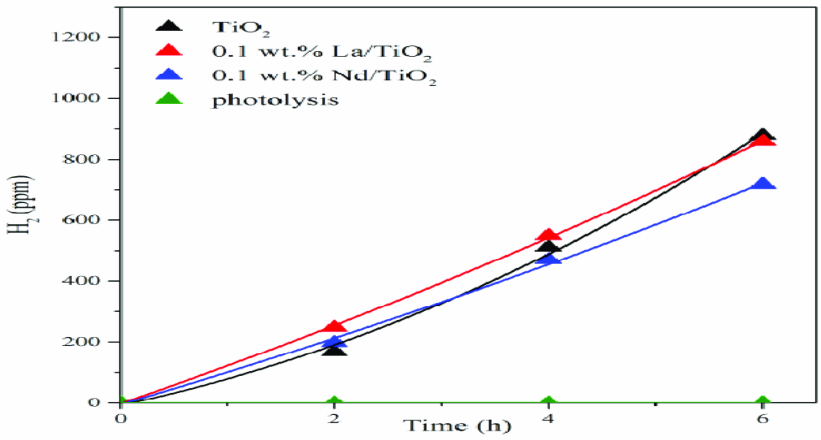

Figure 6. Photocatalytic hydrogen production according to reaction time.

Figure 6: The amount of time needed for photocatalytic hydrogen generation.

Doping with metals like Ag, Cu, Pt, or Au would be another way to improve hydrogen production. This is because these metals are electronegativity, meaning hydrogen likes to stick to them (Eslami, Norouzbahari, Vatanpour, Ghadimi, & Rostamizadeh, 2024).

CONCLUSION:

This study successfully made all suggested catalysts, as shown by the characterizations. With X-ray diffraction, the solid structure of both pure and catalysts can be found. The crystallinity decreased when the oxide was infused into the ZSM-5 zeolite, and the distinct peaks widened. This was because of the titanium dioxide (Ti in the structure. By looking at N2 adsorption and release isotherms, it was possible to determine that zeolite mainly comprises tiny pores. FTIR showed no Ti replacement during the impregnation process in the Si tetrahedral sites.

We used these catalysts to break down synthetic waste using light and to make hydrogen. They were very good at changing colors because the oxide and zeolite worked together. This created a heterojunction that increased the photocatalytic activity, resulting in 100% color change in the first few minutes of the reaction and mineralization of over 95%. When it came to making hydrogen, the same catalysts didn't work as well as when used for photocatalytic degradation. The pure industrial catalyst worked better than the others.

REFERENCES:

1. Adesibikan, A. A., Emmanuel, S. S., Olawoyin, C. O., & Ndungu, P. (2024). Cellulosic Metallic Nanocomposites for Photocatalytic Degradation of Persistent Dye Pollutants in Aquatic Bodies: A Pragmatic Review. *Journal of Organometallic Chemistry*, 123087.
2. Ahlawat, K., Jangra, R., & Prakash, R. (2024). Environmentally Friendly UV-C Excimer Light Source with Advanced Oxidation Process for Rapid Mineralization of Azo Dye in Wastewater. *ACS omega*.
3. Allawi, F., Mahdi, M., Kadhim, M. J., & Alkhayatt, A. H. O. (2024). Preparation and characterization of ZnO/CuO nanocomposite thin films for highly efficient visible-light photocatalysis of acriflavine dye. *Optik*, *303*, 171722.
4. Basavannavar, D. R., Mishra, K. M., Biju, A., Kumar, J. N., Praveen, B., & Nagaraju, G. (2024). Linum usitatissimum mediated green synthesis of Cu3V2O8 nanoparticles and its photocatalytic activity studies. *Environmental Nanotechnology, Monitoring & Management*, *21*, 100912.

5. Chandiran, K., Pandian, M. S., Balakrishnan, S., Pitchaimuthu, S., Chen, Y.-S., & Raja, K. C. N. (2024). Ti3C2Tx MXene decorated with NiMnO3/NiMn2O4 nanoparticles for simultaneous photocatalytic degradation of mixed cationic and anionic dyes. *Colloids and Surfaces A: Physicochemical and Engineering Aspects*, 133888.
6. Chauke, N. M., Mohlala, R. L., Ngqoloda, S., & Raphulu, M. C. (2024). Harnessing visible light: enhancing TiO2 photocatalysis with photosensitizers for sustainable and efficient environmental solutions. *Frontiers in Chemical Engineering, 6*, 1356021.
7. Dhanda, E., Nain, A., & Dahiya, S. (2024). Synthesis of PANI@ Ce-doped ZnO (PCZ) heterojunction: A UV-driven photocatalyst for reduction of Methylene Blue and study of their structural, optical, and electrical properties. *Physica Scripta*.
8. Doan, V.-D., Nguyen, T. T. N., Le Pham, H. A., Nguyen, T. L. H., Lebedeva, O. E., Dang, H. P., . . . Tran, V. A. (2024). Novel photocatalyst for dye degradation: Cu2O/Ag2MoO4 nanocomposite on cellulose fibers from recycled cigarette butts. *Journal of Molecular Liquids*, 124261.
9. Eslami, S., Norouzbahari, S., Vatanpour, V., Ghadimi, A., & Rostamizadeh, M. (2024). Synthesis and characterization of enhanced polysulfone-based mixed matrix membranes containing ZSM-5 zeolite for protein and dye removal. *Journal of Industrial and Engineering Chemistry*.
10. Farahmandzadeh, F., Molaei, M., Salehi, S., & Molahosseini, E. (2024). Simultaneous and fast degradation of methylene blue, methylene orange, and Rhodamine B dyes by high-performance rGO/Fe3O4/ZnSe magnetic nanocomposites. *Colloids and Surfaces A: Physicochemical and Engineering Aspects, 685*, 133229.
11. Gallegos-Cerda, S. D., Hernández-Varela, J. D., Pérez, J. J. C., Huerta-Aguilar, C. A., Victoriano, L. G., Arredondo-Tamayo, B., & Hernández, O. R. (2024). Development of a low-cost photocatalytic aerogel based on cellulose, carbon nanotubes, and TiO2 nanoparticles for degrading organic dyes. *Carbohydrate Polymers, 324*, 121476.
12. Gharbi, A. H., Hemmami, H., Laouini, S. E., Bouafia, A., Ben Amor, I., Zeghoud, S., . . . Abdullah, J. A. A. (2024). Novel CuO–SiO2 nanocomposites: synthesis, kinetics, recyclability, high stability, and photocatalytic efficiency for Rose Bengal dye removal. *Transition Metal Chemistry*, 1-19.

13. Horzum, N., Doğan, D., Karaduman, F. R., & Metin, A. e. l. U. l. (2024). Beyond Conventional: Antibacterial, Antioxidant, and Photocatalytic Properties of Nanofibers Featuring Metal-Oxide-Modified Boron Nitride Nanoparticles. *ACS Applied Polymer Materials*.
14. Kandhasamy, N., Murugadoss, G., Kannappan, T., Kirubaharan, K., Manavalan, R. K., Devanesan, S., . . . Yadav, H. M. (2024). Synthesis of nickel–manganese sulfide decorated with reduced graphene oxide nanocomposite for ultra-fast photocatalytic degradation of organic dye molecules. *Carbon Letters*, *34*(2), 827-840.
15. Krishnan, A., Swarnalal, A., Das, D., Krishnan, M., Saji, V. S., & Shibli, S. (2024). A review on transition metal oxide-based photocatalysts for degradation of synthetic organic pollutants. *Journal of Environmental Sciences, 139*, 389-417.
16. Kumar, P., & Kumar, A. (2024). Multifunctional CoFe2O4/ZnO nanocomposites: probing magnetic and photocatalytic properties. *Nanotechnology, 35*(14), 145705.
17. Lee, D.-E., Danish, M., & Jo, W.-K. (2024). Two birds with one stone: Facile fabrication of a ternary ZnIn2S4/BiVO4/MWCNTs nanocomposite for photocatalytic detoxification of priority organic pollutants and hydrogen production with a proposed mechanism. *Journal of Alloys and Compounds, 980*, 173615.
18. Li, M., Zhang, R., Zou, Z., Zhang, L., & Ma, H. (2024). Optimizing physicochemical properties of hierarchical ZnO/TiO2 nano-film by the novel heating method for photocatalytic degradation of antibiotics and dye. *Chemosphere, 346*, 140392.
19. Liaquat, I., Munir, R., Abbasi, N. A., Sadia, B., Muneer, A., Younas, F., . . . Noreen, S. (2024). Exploring zeolite-based composites in adsorption and photocatalysis for toxic wastewater treatment: Preparation, mechanisms, and future perspectives. *Environmental Pollution*, 123922.
20. Liou, T.-H., Liu, R.-T., Liao, Y.-C., & Ku, C.-E. (2024). Green and sustainable synthesis of mesoporous silica from agricultural biowaste and functionalized with TiO2 nanoparticles for highly photoactive performance. *Arabian Journal of Chemistry*, 105764.
21. Liu, F., Rincón, I., Baldoví, H. G., Dhakshinamoorthy, A., Horcajada, P., Rojas, S., . . . Fateeva, A. (2024). Porphyrin-based MOFs for photocatalysis in water: advancements in solar fuels generation and pollutants degradation. *Inorganic Chemistry Frontiers*.
22. Masho, T. J., Arasu, P. T., Bogale, R. F., Zerrefa, E. A., & Ramamurthy, S. (2024). Green synthesis, characterization of Ag2O/CuO/ZnO nanocomposites using aqueous extract of Croton

macrostachyus leaf for Photodegradation, antimicrobial and antioxidant activities. *Results in Chemistry, 7*, 101369.

23. Nagaraja, K., Arunpandian, M., & Oh, T. H. (2024). Green Synthesis of Platinum Nanoparticles Using Polymer Bio-reduction Approach and Their Photocatalytic Organic Dye Degradation. *Journal of Polymers and the Environment*, 1-12.
24. Patar, S., Mittal, R., Bhuyan, B. K., & Borthakur, L. J. (2024). Fabrication of CoFe2O4/sulfonated graphene oxide antibacterial nanohybrid and evaluation of its enhanced photocatalytic activity, mechanism, and pathway of degradation of textile dyes. *Journal of Water Process Engineering*, *58*, 104795.
25. PETROVIĆ, M., RADIVOJEVIĆ, D., RANČEV, S., Velinov, N., KOSTIĆ, M., BOJIĆ, D., & BOJIĆ, A. (2024). Non-thermal atmospheric-pressure positive pulsating corona discharge in degradation of textile dye Reactive Blue 19 enhanced by Bi2O3 catalyst. *Plasma Science and Technology*, *26*(2), 025504.
26. Pompapathi, K., Anantharaju, K. S., Karuppasamy, P., Subramaniam, M., Uma, B., Boppanahalli Siddegowda, S., . . . Murthy, H. A. (2024). Visible-Light-Driven Mentha spicata L.-Mediated Ag-Doped Bi2Zr2O7 Nanocomposite for Enhanced Degradation of Organic Pollutants, Electrochemical Sensing, and Antibacterial Applications. *ACS Environmental Au*.
27. Prathap, A., Naik, H. B., Viswanath, R., & Vishnu, G. (2024). Biogenic synthesis of Cd doped SrFe2O4 nanoparticles using Datura metal leaves extract and its performance as photocatalytic agent for mixed dyes and electrochemical properties—*Journal of Crystal Growth*, *630*, 127590.
28. Preethi, T., Pachamuthu, M., Senthil, K., Arulmani, S., Pugalmani, S., & Ashokan, S. (2024). Microwave-assisted synthesis of SnO2: ZnO nanocomposites for photocatalytic, antimicrobial, and electrochemical urea detection applications. *Journal of Molecular Structure*, *1304*, 137667.
29. Rohit, M., Reji, R., Singh, H. N., Kumar, J. N., Alarfaj, A. A., Praveen, B., & Nagaraju, G. (2024). Facile green synthesis of Ni3V2O8 nanoparticles for efficient photocatalytic degradation of Rose Bengal dye under visible light irradiation. *Chemical Physics Letters*, 141246.
30. Samal, A., & Das, D. P. An Effective Strategy for the Photocatalytic Elimination of Industrial Wastewaters Via Mgfe-LDH/Tio2 Heterojunctions.
31. Sarvalkar, P. D., Kamble, S. S., Powar, P. S., Kakade, S. S., Jamadar, A. S., Thounaojam, P., . . . Sharma, K. K. K. (2024). Synthesized rGO/f-MWCNT-architectured 1-D ZnO nanocomposites

for azo dyes adsorption, photocatalytic degradation, and biological applications. *Catalysis Communications, 187*, 106846.

32. Sathisha, H., Krishnamurthy, G., Harini, R., & Nagaraju, G. (2024). Facile synthesis of Cu2S-NiS2 nanocomposite with highly active visible light photocatalyst for dye removal and biological evaluation. *Polyhedron*, 116962.
33. Shabna, S., Singh, C. J. C., Dhas, S. D. S. J., Jeyakumar, S. C., & Biju, C. S. (2024). An overview of prominent factors influencing the photocatalytic degradation of cationic crystal violet dye employing diverse nanostructured materials. *Journal of Chemical Technology & Biotechnology*.
34. Shee, N. K., & Kim, H.-J. (2024). Porphyrin-Based Nanomaterials for the Photocatalytic Remediation of Wastewater: Recent Advances and Perspectives. *Molecules*, *29*(3), 611.
35. Shree Lakshmi, K., Soundarya Patel, T., Megha, N., Manohara, G., Babu, N., & Nagaraju, G. (2024). Artemisia Pallens Assisted Synthesis of CeO2–NiO Nanocomposite for Removing Hazardous Rose Bengal Dye and Voltammetric Sensing of Heavy Metals. *Chemistry Africa*, 1-18.
36. Sukarta, I. N., & Sastrawidana, I. (2024). Synthesis and Characterization of Hydroxyapatite/Titania Composite and Its Application on Photocatalytic Degradation of Remazol Red B Textile Dye Under UV Irradiation. *Ecological Engineering & Environmental Technology (EEET), 25*(2).
37. Survase, A. A., & Kanase, S. S. (2024). Novel microbial synthesis of rGO nanosheets for effective photocatalytic remediation of Acid Blue 113 dye, improved seed germination, antimicrobial and antioxidant applications—*Journal of Molecular Structure, 1302*, 137421.
38. Wani, A. A., Rather, R. A., Shaari, N., Khan, U., Muhammad, T., Hussain, S. M., & Abed, A. M. (2024). Aspects of superior photocatalytic dye degradation and adsorption efficiency of reduced graphene oxide multiwalled carbon nanotubes with modified ZnO-Al2O3 nanocomposites. *Journal of Environmental Chemical Engineering*, 112461.
39. Xu, L., Guo, P., Xu, J., Shen, B., & Zhao, Z. (2024). Regulation of TiO2/ZSM-5 catalyst for enhanced photocatalytic toluene oxidation: Intensified light absorption, charge separation, and toluene adsorption. *Colloids and Surfaces A: Physicochemical and Engineering Aspects*, 133832.

40. Yan, B., Dai, Y., Xin, L., Li, M., Zhang, H., Long, H., & Gao, X. (2024). Research progress in the degradation of printing and dyeing wastewater using chitosan-based composite photocatalytic materials. *International Journal of Biological Macromolecules*, 130082.